

1 **Determination of silt loading distribution characteristics**
2 **using a rapid silt loading testing system in Tianjin, China**

3 **Wei Zhang, Yaqin Ji* , Shijian Zhang, Lei Zhang, Shibao Wang**

4 College of Environmental Science and Engineering, Nankai University, Tongyan
5 Road 38#, Haihe Education Park, Jinnan District, Tianjin, CN, 300350

6 **Abstract:** Silt loading (sL) is an important parameter in the fugitive road dust (FRD)
7 emission inventory because it can indicate the cleaning degree of roads. In this study,
8 we combined Testing Re-entrained Aerosol Kinetic Emissions from Roads (TRAKER)
9 with the AP-42 method to measure the sL values of paved roads in Tianjin, China, and
10 we developed a rapid silt loading testing system for the period from January to
11 October in 2015. This allowed us to establish the FRD sL reservoir in a more feasible
12 manner on a larger urban scale compared with sL measurements alone. We found that
13 the background-corrected TRAKER signals tended to increase slightly as the speed of
14 the mobile monitoring system increased, and the sL values increased exponentially
15 with the speed-corrected TRAKER signals. The sL values determined by TRAKER
16 were quite different, where branch roads > minor arterials > major arterials > outer
17 ring > expressway, due to differences in the average speed and traffic volume.
18 Furthermore, the sL values determined using TRAKER were higher in the slow lanes
19 than the other lanes (except for the outer ring), whereas the sL values produced by
20 TRAKER in the express lanes of the outer ring were the highest among all the vehicle
21 lanes. The frequency distribution of the sL values obtained by TRAKER for various
22 types of roads differed significantly from each other in terms of magnitude, especially
23 on the branch roads and minor arterials. In terms of the temporal distribution, the sL
24 values obtained by TRAKER were substantially higher in summer, followed by spring
25 and autumn, and lowest in winter.

26 **Keywords:** AP-42, silt loading, Tianjin, TRAKER.

*Corresponding author. Tel: +86-022-23503397; Fax: +86-22-23503397

| E-mail address: jiyaqin@nankai.edu.cn

27 Introduction

28 The recent rapid economic growth in China has been accompanied by a severe
29 particulate matter pollution problem. In particular, fugitive dust has attracted much
30 attention in China because it is one of the main sources of particulate matter (Long et
31 al., 2016; Tian et al., 2016). Fugitive road dust (FRD) is an important type of fugitive
32 dust in cities (Amato et al., 2009b; Etyemezian et al., 2003; Li et al., 2016) and one of
33 the major contributors to particulate matter (Amato et al., 2012; Amato et al., 2009a;
34 Athanasopoulou et al., 2010; Cheng et al., 2007; Karanasiou et al., 2011;
35 Martuzevicius et al., 2011; Sun et al., 2004; Thorpe and Harrison, 2008; Zhao et al.,
36 2016; Zhao et al., 2006). Furthermore, the contribution of FRD to the total PM_{2.5}
37 emissions is about 20% (Gao et al., 2016; Hsu et al., 2016; Karagulian et al., 2015;
38 Liu et al., 2015). FRD not only affects the air quality and visibility (Almeida et al.,
39 2006; Amato et al., 2016; Borrego et al., 2016; Cyrus et al., 2014; Liu et al., 2014;
40 Moreno et al., 2013), but it is also highly detrimental to health (Huang et al., 2014;
41 Lai et al., 2016; Lu et al., 2009; Tente et al., 2011). Thus, controlling and quantifying
42 the particulate matter emissions produced by vehicle traffic and resuspended on roads
43 is essential for understanding the potential emissions of particulate pollution, thereby
44 establishing foundations for environmental management and managing the air quality
45 by implementing particle matter (PM) reduction measures (Amato F, 2010;
46 Etyemezian et al., 2003; Kavouras et al., 2016).

47 Silt loading (sL) is a very important parameter in the FRD emission inventory
48 and thus for environmental management. The AP-42 method (i.e., vacuuming and
49 sweeping) specified by the EPA has been employed by many researchers to study
50 FRD emissions, including emission inventories, emission characteristics, and the
51 efficiency of control measures (Shou-bin et al., 2009). However, this method is not
52 practicable for measuring sL at a regional scale because of time constraints and safety
53 problems. In particular, it cannot precisely reflect the actual situation regarding the
54 resuspension of FRD due to vehicular travel because the resuspension mechanism
55 assumed for FRD might not be the same as that due to actual vehicular travel (Han et
56 al., 2011).

57 Therefore, in this study, we developed a rapid silt loading testing system by
58 combining Testing Re-entrained Aerosol Kinetic Emissions from Roads (TRAKER)
59 with the AP-42 method to detect the silt loading on roads in Tianjin, China. The
60 TRAKER system was first tested in Las Vegas, USA by Kuhns et al. (Kuhns et al.,
61 2001). Subsequently, it was used to assess the quantitative relationships among the
62 key factors that generate road particle emissions (Hussein et al., 2008). Kwak et al.
63 also utilized TRAKER to investigate the physical and chemical characteristics of
64 ultrafine particles in Hwaseong, South Korea (Kwak et al., 2014).

65 The new system has several advantages, as follows: (1) the dust emissions from
66 long stretches and numerous roads can potentially be surveyed in a quantitative
67 manner within a short time (Han and Jung, 2012; Kuhns et al., 2001); (2) the results
68 obtained by this system can reflect the actual FRD resuspension mechanism due to
69 vehicles; (3) the system can perform tasks that are not possible using AP-42 alone and
70 it is more flexible on an urban scale.

71 Road dust pollution is an important issue in Tianjin because of its high volume of
72 vehicles. Various studies in this field have concentrated mostly on the FRD emission
73 characteristics or its chemical components (Hussein et al., 2008; Kauhaniemi et al.,
74 2014; Kwak et al., 2014; Shou-bin et al., 2009; Zhu et al., 2009), whereas few studies
75 have considered the spatial and temporal variations in important parameters in the
76 FRD emission inventory.

77 In this study, we obtained the first experimental estimates of sL using a rapid silt
78 loading testing system in Tianjin. The main objective of this study was to obtain the
79 sL values for all of the roads sampled by combining TRAKER with the AP-42 method.
80 The secondary objective was to determine the spatial and temporal distribution
81 characteristics of the sL values obtained by TRAKER. The final objective was to
82 provide an experimental basis for measuring emission factors and emissions for FRD
83 due to vehicle movements, thereby establishing an emissions inventory for FRD.

84 2. Experimental methods

85 2.1. Particle concentration monitoring system

86 A schematic of the sampling system is shown in Figure 1. The vehicle used in

87 this experiment was a four-door, four-wheel Ford Maverick vehicle (2012) with a curb
88 weight of 2092 kg. The vehicle was equipped with a global positioning system (GPS)
89 receiver and two DustTrak particle monitors with a 2.5 μm size selective inlet. The
90 DustTrak particle monitor (model #8530, TSI Company, USA) is a portable
91 instrument for measuring the concentrations of different particle sizes in real time.
92 Before starting a test, all of the instruments were synchronized with the time reported
93 by the GPS.

94 The two inlet lines of DustTrak entered the compartment of the sports-utility
95 vehicle through the car windows, where the lines were 9 mm in diameter and 2.0 m in
96 length. One inlet of the tire line on the right was 175 mm above the ground and 50
97 mm behind the tire. Measurements obtained behind the tire while moving indicated
98 that the air speed along the center of the tire was not influenced significantly by the
99 ambient wind direction at distances less than 100 mm from the tire (Etyemezian et al.,
100 2003). Another inlet was placed on the roof to test the background concentrations,
101 whereas it was laid above the hood of the vehicle in a previous study (Kuhns et al.,
102 2001) or on the front bumper (Han et al., 2011). This could reduce the effects of other
103 vehicles on the background concentration.

104 The DustTrak data obtained from both the roof and tire-mounted instruments
105 were combined with the GPS data based on their common time variables. Each 1-s
106 TRAKER data set was considered to be valid if the following criteria were satisfied:
107 (1) the maximum threshold for acceleration and deceleration was 0.5 m/s^2 . Braking
108 and hard acceleration or deceleration could emit a high concentration of particulate
109 matter instantly; (2) when the vehicle speed (measured by the GPS) was less than 5
110 km/h, it was assumed that the TRAKER signal was insignificant and the data were
111 invalid; (3) the maximum threshold for the wheel angle with respect to the body of the
112 vehicle was 3° , which ensured that the orientation of the TRAKER inlets with respect
113 to the front tire did not change during the measurements (Etyemezian et al., 2003).

114 2.2. Speed response

115 The variation in the TRAKER signals with vehicle speed was assessed during
116 testing on paved roads in Tianjin. A straight 1200-m section of road was covered in

117 both the eastbound and westbound directions. According to the maximum speed in the
118 urban area (80 km/h) and the minimum threshold speed reported previously (5 m/s)
119 (Etyemezian, 2003), four passes were completed at each speed (10, 15, 20, 25, 30, 35,
120 40, 45, 50, 55, 60, 65, 70, 75, and 80 km/h) with a total of 60 passes. The TRAKER
121 signals obtained from the DustTrak were averaged for each pass.

122 2.3. *sL* sampling system

123 In addition to TRAKER measurements, samples were collected from nine paved
124 road sites during four seasons. At each site, four sections of the sampled roads were
125 measured, marked, and vacuumed using an 800-W vacuum cleaner, 1 m² sampling
126 frame, fine wool brush, 3-kw gasoline generator, and a handheld GPS receiver. The
127 samples were weighed and sieved using a 200-mesh standard Taylor screen, a “one
128 over ten thousand” electronic balance, and an electric vibration sieve machine. The
129 nine paved roads comprised one expressway, one outer ring, two major arterial roads,
130 two minor arterial roads, and three branch roads. Table 1 shows the details of the nine
131 typical road sites.

132 The rapid silt loading testing system was applied in the Tianjin urban area from
133 January to October in 2015. Tianjin is a typical northern city with the monsoon
134 climate found in the medium latitudes on the North China Plain, and thus January was
135 a representative month in winter (December to February), and April, July, and
136 October were representative months in spring (March to May), summer (June to
137 August), and autumn (September to November), respectively. Therefore, sampling
138 was conducted in January, April, July, and October.

139 3. Results

140 3.1. Relationship between vehicle speed and background-corrected TRAKER signals

141 Sixty data points were obtained in the speed response experiment described in
142 Section 2.3. Figure 2 shows the relationship between the background-corrected
143 TRAKER signals (T , mg/m³) and vehicle speed (s , km/h), where each point represents
144 the average value obtained by the TRAKER signal. T is the background-corrected
145 TRAKER signal, which was obtained by subtracting the background-corrected values
146 (mg/m³) from the TRAKER signals measured behind the tire. The

147 background-corrected values were obtained by subtracting the average TRAKER
148 signals at a speed of 0 km/h from the background TRAKER signals. This accounted
149 for particle losses within the TRAKER inlet lines, dust or exhaust emissions
150 generated by other vehicles close to the TRAKER vehicle on the road, ambient wind,
151 and inter-instrument bias. And the background-corrected values ranged from 0.000 to
152 0.012 mg/m³.

153 Figure 2 demonstrates that the background-corrected TRAKER signals increased
154 with the vehicle speed over the same segment of road. The quantitative relationship
155 between the background-corrected TRAKER signal and the vehicle speed was
156 exponential, with a correlation coefficient (R^2) of 0.95 (about 95% of the variances in
157 the signals were explained by the vehicle's speed). The correlations obtained by
158 Etyemezian et al. (Etyemezian et al. ; 2003) between PM₁₀ signals and vehicle speed
159 in Treasure Valley and Ft Bliss speed tests were $T = 0.00017*s^{2.96}$ ($R^2 = 0.972$) and
160 $T = 0.00012*s^{2.76}$ ($R^2 = 0.923$), respectively. There were some differences in these
161 correlations, which may have been caused by the diverse silt and surface
162 characteristics of the road sections sampled in the two studies. Therefore, when sL is
163 measured in a specific area, the calibration procedure is essential in order to make the
164 correlation equation applicable exclusively to local paved roads.

165 To remove the speed-dependent variable, the equation in Figure 2 was
166 transformed into another formula (formula (1)), where the average
167 background-corrected TRAKER signals were adjusted to a speed of 40 km/h. We
168 selected 40 km/h as the normalizing variable because this was the average speed
169 during sampling.

$$170 \quad T^* = \left(\frac{40}{s}\right)^{2.5717} * T \quad (1)$$

171 Where T is the background-corrected TRAKER signal in mg/m³, s is the vehicle
172 speed in the conventional units of km/h, and T^* is the speed-corrected TRAKER
173 signal.

174 3.2. Relationship between the speed-corrected TRAKER signals and sL values

175 The regression equations obtained using the sL values (y) and speed-corrected

176 TRAKER signals (x) in the four seasons are shown in Figure 3, which indicates that
177 the sL values increased exponentially with the speed-corrected TRAKER signals. The
178 R^2 values for the four seasons were 0.901, 0.766, 0.584, and 0.768 respectively, which
179 suggests that about 90%, 77%, 58%, and 77% of the variation in sL could be
180 explained by the speed-corrected TRAKER signals in the four seasons, respectively.
181 The equations presented in Figure 3 were used to estimate the sL values based on the
182 speed-corrected TRAKER signals on the scale of the whole study area. These results
183 allowed us to establish the FRD sL reservoir in a more feasible manner on a higher
184 geographic scale than that using sL measurements alone.

185 3.3. Spatial distribution characteristics of sL values obtained by TRAKER and its
186 impact factors

187 3.3.1 Distribution characteristics of the sL values obtained by TRAKER for different
188 types of roads and its impact factors

189 Figure 4 shows the trends in the sL values obtained by TRAKER for various
190 types of roads. As shown in Figure 4, the average sL values obtained by TRAKER on
191 different types of roads were 0.49 g/m^2 for branch roads, 0.30 g/m^2 for minor arterials,
192 0.29 g/m^2 for major arterials, 0.26 g/m^2 for the outer ring, and 0.09 g/m^2 for the
193 expressway. The maximum value (for branch roads) was five times the minimum (for
194 the expressway) and there were obvious differences among the various types of roads.
195 The average speeds on the different types of roads were as follows: expressway
196 (53.72 km/h) > outer ring (48.69 km/h) > major arterials (36.42 km/h) > minor
197 arterials (31.35 km/h) > branch roads (25.14 km/h). The trends in the traffic volumes
198 were the same as the average speed on the different types of roads, as shown in Table
199 2, so the traffic volume on the expressway was the maximum among all the types of
200 roads in Tianjin. By contrast, the minimum traffic volume was found on the branch
201 roads. Thus, the volume and speed were relatively lower on the branch roads than the
202 others, so the FRD was more easily produced and its value was the maximum among
203 all the types of roads. In addition, more crossings contributed to the maximum on
204 branch roads because they led to more turning, braking, and starting, thereby
205 increasing the maximum sL values determined by TRAKER. The main explanation

206 for the minimum sL values on expressways was the higher traffic volume and average
207 speed compared with the others, which led to a higher resuspension rate for the
208 particles deposited on the road. There may also have been no major soil dust sources
209 near the expressways, thereby leading to the minimum sL values determined by
210 TRAKER. In addition, heavy trucks used for construction or transportation were
211 found rarely on the expressway. In conclusion, the traffic volume and average speed
212 were the major contributors to the sL values, but other factors could have influenced
213 the sL values such as the road materials and road conditions (Zhu et al., 2012). These
214 results suggest that the sL values obtained by TRAKER were inversely proportional to
215 both the average speed and traffic volume.

216 Based on those results, control measures such as increasing the cleaning
217 frequency should be taken to prevent the resuspension of FRD and to maintain a clean
218 and tidy road.

219 3.3.2 Distribution characteristics of the sL values obtained by TRAKER in different 220 vehicle lanes

221 The sL values obtained by TRAKER in different vehicle lanes on various types
222 of roads in Tianjin are shown in Figure 6. A schematic diagram illustrating the different
223 vehicle lanes on roads in Tianjin is shown in Figure 5. Figure 6 shows that the sL
224 values obtained by TRAKER in slow lanes were higher than those in the other lanes
225 (except for the outer ring), which may be associated with the minimum traffic volume
226 and average speed in slow lanes. Figure 6 shows clearly that there were no significant
227 differences among lanes on the expressway (except for the slow lane), which might
228 have been associated with their similar speed. However, the outer ring was a special
229 type of road, where the traffic volume and speed did not differ significantly between
230 lanes. Furthermore, erosion due to rain and wind sent dust from the green belts into
231 the nearby express lane, so the sL values obtained by TRAKER in this lane were
232 higher than those in the others (Figure 6). Thus the traffic volume and average speed
233 were the main factors that affected the distribution of the sL values obtained by
234 TRAKER in different lanes, as suggested previously (Han and Jung, 2012)

235 3.4 Frequency distribution of sL values obtained by TRAKER on different types of

236 roads

237 Figure 7 shows the frequency distribution of the sL values obtained by
238 TRAKER on different types of roads. According to Figure 7, the sL values
239 determined by TRAKER on different types of roads were clearly quite different,
240 especially on branch roads and minor arterials. For branch roads, about 34% of the
241 sL values obtained by TRAKER were less than 0.2 g/m^2 and about 5% were more
242 than 1.0 g/m^2 . For minor arterials, about 46% of the sL values obtained by TRAKER
243 were less than 0.2 g/m^2 and very few of the sL values were more than 1.0 g/m^2 . For
244 the five types of roads in Tianjin, the percentage of sL values obtained by TRAKER
245 ($<0.2 \text{ g/m}^2$) on the expressway was relatively higher than that on any of the other
246 types of roads (82%). Outer ring had the next highest percentage (60%), followed by
247 major arterials (52%) and minor arterials (46%). The percentage of sL values
248 obtained by TRAKER ($<0.2 \text{ g/m}^2$) was the lowest on branch roads (34%). Due to the
249 high percentage range of sL values obtained by TRAKER ($<0.2 \text{ g/m}^2$) on different
250 types of roads, many samples are required to ensure that accurate estimates are
251 produced for sL . The results indicate that the frequency distribution of the sL
252 values obtained by TRAKER was mainly related to the traffic volume and average
253 speed.

254 The different frequency distributions indicated that there were significant
255 differences among the types of roads and many measurements were needed to
256 accurately estimate the sL values on an urban scale. The AP-42 method measures the
257 sL based on a scale of only a small part of the road, thereby leading to greater
258 uncertainty compared with the results obtained by TRAKER. Thus, the AP-42
259 method will lead to more uncertainty regarding the emission factors, and thus the
260 emissions inventory.

261 3.5 Temporal distribution of sL values by TRAKER and its impact factors

262 The temporal distributions of the sL values obtained by TRAKER in different seasons
263 are presented in Figure 8, which suggests that there were seasonal differences among
264 the sL values produced by TRAKER. The sL values obtained by TRAKER in summer
265 were relatively higher than those in any of the other seasons (0.37 g/m^2). Spring was

266 the next highest season (0.33 g/m^2), followed by autumn (0.26 g/m^2) and winter (0.24
267 g/m^2). As shown in Figure 8, the days when the rainfall exceeded 0.254 mm in the
268 four seasons followed the trend of: summer > autumn > spring > winter. The highest
269 amount of rainfall in the summer meant that the vehicle tires readily distributed mud
270 on the road surfaces, thereby increasing the sL values for the road surface. Moreover,
271 rainfall increased the accumulation of soil particles on the road in rainwater from soil
272 sources adjacent to the road during the summer. The minimum sL values obtained by
273 TRAKER in the winter may be explained by the higher wind speed in the winter
274 among the four seasons, thereby increasing the FRD. Furthermore, the decreased
275 fallout phenomenon during vehicle movements may be a factor that accounted for the
276 minimum sL values obtained by TRAKER. Therefore, the temporal distribution of the
277 sL values obtained by TRAKER in different seasons may be related to many factors,
278 such as temperature, humidity, rainfall, wind speed, and wind direction. Thus, more
279 measures should be implemented, such as vacuum street sweeping and water spraying
280 (Yuan C S et al, 2003), to reduce the FRD levels during the summer and spring
281 compared with the other two seasons.

282 4. Conclusions

283 This study obtained the first experimental estimations of road dust sL by using a
284 rapid silt loading testing system in Tianjin. The rapid silt loading testing system
285 combined TRAKER with AP-42, and it was implemented between January and
286 October 2015 in Tianjin. The sL values were measured on typical roads during four
287 seasons. After collecting sufficient data to determine the sL values using TRAKER,
288 we determined the spatial and temporal distributions characteristics of the sL values,
289 which allowed us to establish the FRD sL reservoir in a more feasible manner on an
290 urban scale than that based on sL measurements obtained by AP-42 alone. This rapid
291 silt loading testing system allows hot spots to be located easily and rapidly.

292 The background-corrected differential TRAKER signals increased slightly as the
293 speed of the mobile monitoring system increased, and the sL values increased
294 exponentially with the speed-corrected TRAKER signals. The sL values obtained by
295 TRAKER were quite different among road types, i.e., branch roads > minor arterials >

296 major arterials > outer ring > expressway, and they were inversely proportional to
297 both the average speed and traffic volume. Furthermore, the *sL* values obtained by
298 TRAKER in slow lanes were higher than those in the other lanes (except for the outer
299 ring road), and the *sL* values obtained by TRAKER in the express lanes of the outer
300 ring were the highest among all the vehicle lanes. The frequency distributions of the
301 *sL* values obtained by TRAKER were quite different among all types of roads in this
302 study. Overall, our findings demonstrate that the traffic volume and average speed on
303 roads were the main factors that determined the distribution characteristics of the *sL*
304 values obtained by TRAKER.

305 The *sL* values obtained by TRAKER in the summer were substantially higher
306 than those in the other seasons. Spring was the next highest season, followed by
307 autumn and winter. These differences may have been associated with the temperature,
308 humidity, rainfall, wind speed, wind direction, and other meteorological factors.

309 310 Acknowledgments

311 This study was funded by “Study on the measurement and emission detection of
312 Road Dust in Beijing-Tianjin-Hebei Area” (2014-2016 Special Environmental
313 Research Fund for Public Welfare, No. 201409004) from the Ministry of
314 Environmental Protection of the People’s Republic of China.

315 316 References

- 317 Almeida, S.M., Pio, C.A., Freitas, M.C., Reis, M.A., Trancoso, M.A.(2006). Source apportionment of atmospheric
318 urban aerosol based on weekdays/weekend variability: evaluation of road re-suspended dust contribution. *Atmos.*
319 *Environ.* 40: 2058-2067.
- 320 Amato, F., Favez, O., Pandolfi, M., Alastuey, A., Querol, X., Moukhtar, S., Bruge, B., Verlhac, S., Orza, J.A.G.,
321 Bonnaire, N., Le Priol, T., Petit, J.F., Sciare, J.(2016). Traffic induced particle resuspension in Paris: Emission
322 factors and source contributions. *Atmos. Environ.* 129: 114-124.
- 323 Amato, F., Karanasiou, A., Moreno, T., Alastuey, A., Orza, J.A.G., Lumbreras, J., Borge, R., Boldo, E., Linares, C.,
324 Querol, X.(2012). Emission factors from road dust resuspension in a Mediterranean freeway. *Atmos. Environ.* 61:
325 580-587.
- 326 Amato, F., Pandolfi, M., Escrig, A., Querol, X., Alastuey, A., Pey, J., Perez, N., Hopke, P.K.(2009a). Quantifying
327 road dust resuspension in urban environment by Multilinear Engine: A comparison with PMF2. *Atmos. Environ.*
328 43: 2770-2780.
- 329 Amato, F., Pandolfi, M., Viana, M., Querol, X., Alastuey, A., Moreno, T.(2009b). Spatial and chemical patterns of

330 PM10 in road dust deposited in urban environment. *Atmos. Environ.* 43: 1650-1659.

331 Amato F, Nava S, Lucarelli F, Querol X, Alastuey A, Baldasano J M, Pandolfi M, (2010). A comprehensive
332 assessment of PM emissions from paved roads: Real-world Emission Factors and intense street cleaning trials.
333 *Science of the Total Environment*, 408(20):4309-18.

334 Athanasopoulou, E., Tombrou, M., Russell, A.G., Karanasiou, A., Eleftheriadis, K., Dandou, A.(2010).
335 Implementation of road and soil dust emission parameterizations in the aerosol model CAMx: Applications over
336 the greater Athens urban area affected by natural sources. *J.Geophys.Res-Atmos.* 115.

337 Borrego, C., Amorim, J.H., Tchepel, O., Dias, D., Rafael, S., Sá, E., Pimentel, C., Fontes, T., Fernandes, P., Pereira,
338 S.R., Bandeira, J.M., Coelho, M.C.(2016). Urban scale air quality modelling using detailed traffic emissions
339 estimates. *Atmos. Environ.* 131: 341-351.

340 Cheng, S., Chen, D., Li, J., Wang, H., Guo, X.(2007). The assessment of emission-source contributions to air
341 quality by using a coupled MM5-ARPS-CMAQ modeling system: A case study in the Beijing metropolitan region,
342 China. *Environ Modell & Softw.* 22: 1601-1616.

343 Cyrys, J., Peters, A., Soentgen, J., Wichmann, H.E.(2014). Low emission zones reduce PM10 mass concentrations
344 and diesel soot in German cities. *J Air & Waste Manage.* 64: 481-487.

345 Etyemezian, V.(2003). Vehicle-based road dust emission measurement (III): effect of speed, traffic volume,
346 location, and season on PM10 road dust emissions in the Treasure Valley, ID. *Atmos. Environ.* 37: 4583-4593.

347 Etyemezian, V., Kuhns, H., Gillies, J., Green, M., Pitchford, M., Watson, J.(2003). Vehicle-based road dust
348 emission measurement: I—methods and calibration. *Atmos. Environ.* 37: 4559-4571.

349 Gao, J., Peng, X., Chen, G., Xu, J., Shi, G.-L., Zhang, Y.-C., Feng, Y.-C.(2016). Insights into the chemical
350 characterization and sources of PM_{2.5} in Beijing at a 1-h time resolution. *Sci.Total Environ.* 542, Part A, 162-171.

351 Han, S., Jung, Y.W.(2012). A study on the characteristics of silt loading on paved roads in the Seoul metropolitan
352 area using a mobile monitoring system. *J Air & Waste Manage.* 62: 846-862.

353 Han, S., Youn, J.-S., Jung, Y.-W.(2011). Characterization of PM₁₀ and PM_{2.5} source profiles for resuspended road
354 dust collected using mobile sampling methodology. *Atmos. Environ.* 45: 3343-3351.

355 Hsu, C.-Y., Chiang, H.-C., Lin, S.-L., Chen, M.-J., Lin, T.-Y., Chen, Y.-C.(2016). Elemental characterization and
356 source apportionment of PM₁₀ and PM_{2.5} in the western coastal area of central Taiwan. *Sci.Total Environ.* 541:
357 1139-1150.

358 Huang, R.J., Zhang, Y.L., Bozzetti, C., Ho, K.F., Cao, J.J., Han, Y.M., Daellenbach, K.R., Slowik, J.G., Platt, S.M.,
359 Canonaco, F., Zotter, P., Wolf, R., Pieber, S.M., Brunns, E.A., Crippa, M., Ciarelli, G., Piazzalunga, A.,
360 Schwikowski, M., Abbaszade, G., Schnelle-Kreis, J., Zimmermann, R., An, Z.S., Szidat, S., Baltensperger, U., El
361 Haddad, I., Prevot, A.S.H.(2014). High secondary aerosol contribution to particulate pollution during haze events
362 in China. *Nature* .514: 218-222.

363 Hussein, T., Johansson, C., Karlsson, H., Hansson, H.-C.(2008). Factors affecting non-tailpipe aerosol particle
364 emissions from paved roads: On-road measurements in Stockholm, Sweden. *Atmos. Environ.* 42: 688-702.

365 Karagulian, F., Belis, C.A., Dora, C.F.C., Prüss-Ustün, A.M., Bonjour, S., Adair-Rohani, H., Amann, M.(2015).
366 Contributions to cities' ambient particulate matter (PM): A systematic review of local source contributions at global
367 level. *Atmos. Environ.* 120: 475-483.

368 Karanasiou, A., Moreno, T., Amato, F., Lumberras, J., Narros, A., Borge, R., Tobias, A., Boldo, E., Linares, C., Pey,
369 J., Reche, C., Alastuey, A., Querol, X.(2011). Road dust contribution to PM levels – Evaluation of the effectiveness
370 of street washing activities by means of Positive Matrix Factorization. *Atmos. Environ.* 45: 2193-2201.

371 Kauhaniemi, M., Stojiljkovic, A., Pirjola, L., Karppinen, A., Harkonen, J., Kupiainen, K., Kangas, L., Aarnio,
372 M.A., Omstedt, G., Denby, B.R., Kukkonen, J.(2014). Comparison of the predictions of two road dust emission
373 models with the measurements of a mobile van. *Atmos Chem and Phys.* 14: 9155-9169.

374 Kavouras, I.G., DuBois, D.W., Nikolich, G., Corral Avittia, A.Y., Etyemezian, V.(2016). Particulate dust emission
375 factors from unpaved roads in the U.S.–Mexico border semi-arid region. *J Arid Environ.*124: 189-192.

376 Kuhns, H., Etyemezian, V., Landwehr, D., MacDougall, C., Pitchford, M., Green, M.(2001). Testing Re-entrained
377 Aerosol Kinetic Emissions from Roads : a new approach to infer silt loading on roadways. *Atmos. Environ.* 35:
378 2815-2825.

379 Kwak, J., Lee, S., Lee, S.(2014). On-road and laboratory investigations on non-exhaust ultrafine particles from the
380 interaction between the tire and road pavement under braking conditions. *Atmos. Environ.* 97:195-205.

381 Lai, S., Zhao, Y., Ding, A., Zhang, Y., Song, T., Zheng, J., Ho, K.F., Lee, S.-c., Zhong, L.(2016). Characterization
382 of PM_{2.5} and the major chemical components during a 1-year campaign in rural Guangzhou, Southern China.
383 *Atmos Res* 167: 208-215.

384 Li, N., Long, X., Tie, X., Cao, J., Huang, R., Zhang, R., Feng, T., Liu, S., Li, G.(2016). Urban dust in the
385 Guanzhong basin of China, part II: A case study of urban dust pollution using the WRF-Dust model. *Sci.Total*
386 *Environ.*541: 1614-1624.

387 Liu, E., Yan, T., Birch, G., Zhu, Y.(2014). Pollution and health risk of potentially toxic metals in urban road dust in
388 Nanjing, a mega-city of China. *Sci.Total Environ.*476–477: 522-531.

389 Liu, G., Li, J., Wu, D., Xu, H.(2015). Chemical composition and source apportionment of the ambient PM_{2.5} in
390 Hangzhou, China. *Particuology* 18: 135-143.

391 Long, X., Li, N., Tie, X., Cao, J., Zhao, S., Huang, R., Zhao, M., Li, G., Feng, T.(2016). Urban dust in the
392 Guanzhong Basin of China, part I: A regional distribution of dust sources retrieved using satellite data. *Sci.Total*
393 *Environ.*541:1603-1613.

394 Lu, X., Li, L.Y., Wang, L., Lei, K., Huang, J., Zhai, Y.(2009). Contamination assessment of mercury and arsenic in
395 roadway dust from Baoji, China. *Atmos. Environ.* 43: 2489-2496.

396 Martuzevicius, D., Kliucininkas, L., Prasauskas, T., Krugly, E., Kauneliene, V., Strandberg, B.(2011).
397 Resuspension of particulate matter and PAHs from street dust. *Atmos. Environ.* 45: 310-317.

398 Moreno, T., Karanasiou, A., Amato, F., Lucarelli, F., Nava, S., Calzolari, G., Chiari, M., Coz, E., Artiñano, B.,
399 Lumbreras, J., Borge, R., Boldo, E., Linares, C., Alastuey, A., Querol, X., Gibbons, W.(2013). Daily and hourly
400 sourcing of metallic and mineral dust in urban air contaminated by traffic and coal-burning emissions. *Atmos.*
401 *Environ.* 68: 33-44.

402 Shou-bin, F., Gang, T., Gang, L., Yu-hu, H., Jian-ping, Q., Shui-yuan, C.(2009). Road fugitive dust emission
403 characteristics in Beijing during Olympics Game 2008 in Beijing, China. *Atmos. Environ.* 43: 6003-6010.

404 Sun, Y., Zhuang, G., Wang, Y., Han, L., Guo, J., Dan, M., Zhang, W., Wang, Z., Hao, Z.(2004). The air-borne
405 particulate pollution in Beijing—concentration, composition, distribution and sources. *Atmos. Environ.* 38:
406 5991-6004.

407 Tente, H., Gomes, P., Ferreira, F., Amorim, J.H., Cascão, P., Miranda, A.I., Nogueira, L., Sousa, S.(2011).
408 Evaluating the efficiency of Diesel Particulate Filters in high-duty vehicles: Field operational testing in Portugal.
409 *Atmos. Environ.* 45: 2623-2629.

410 Thorpe, A., Harrison, R.M.(2008). Sources and properties of non-exhaust particulate matter from road traffic: A
411 review. *Sci.Total Environ.*400: 270-282.

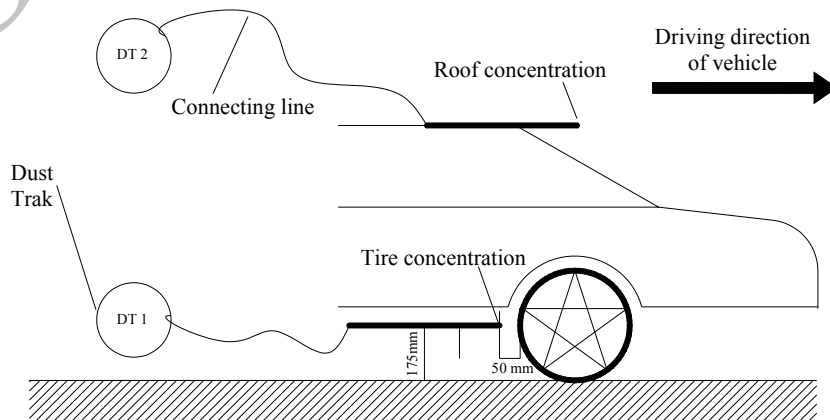
412 Tian, Y.-Z., Chen, G., Wang, H.-T., Huang-Fu, Y.-Q., Shi, G.-L., Han, B., Feng, Y.-C.(2016). Source regional
413 contributions to PM_{2.5} in a megacity in China using an advanced source regional apportionment method.
414 *Chemosphere* 147: 256-263.

415 Yuan C S, Cheng S W, Hung C H, Yu T Y.(2003). Influence of Operating Parameters on the Collection Efficiency
416 and Size Distribution of Street Dust during Street Scrubbing. *Aerosol & Air Quality Research*, 3(1):75-81.

417 Zhao, H., Shao, Y., Yin, C., Jiang, Y., Li, X.(2016). An index for estimating the potential metal pollution

418 contribution to atmospheric particulate matter from road dust in Beijing. *Sci.Total Environ.*550: 167-175.
419 Zhao, P., Feng, Y., Zhu, T., Wu, J.(2006). Characterizations of resuspended dust in six cities of North China. *Atmos.*
420 *Environ.* 40: 5807-5814.
421 Zhu, D., Kuhns, H.D., Brown, S., Gillies, J.A., Etyemezian, V., Gertler, A.W.(2009). Fugitive Dust Emissions from
422 Paved Road Travel in the Lake Tahoe Basin. *J. Air & Waste Manage.* 59: 1219-1229.
423 Zhu D, Kuhns H D, Gillies J A, Etyemezian V, Brown S, Gertler A W.(2012). Analysis of the effectiveness of
424 control measures to mitigate road dust emissions in a regional network. *Transportation Research Part D Transport*
425 *& Environment*, 17(4):332-340.

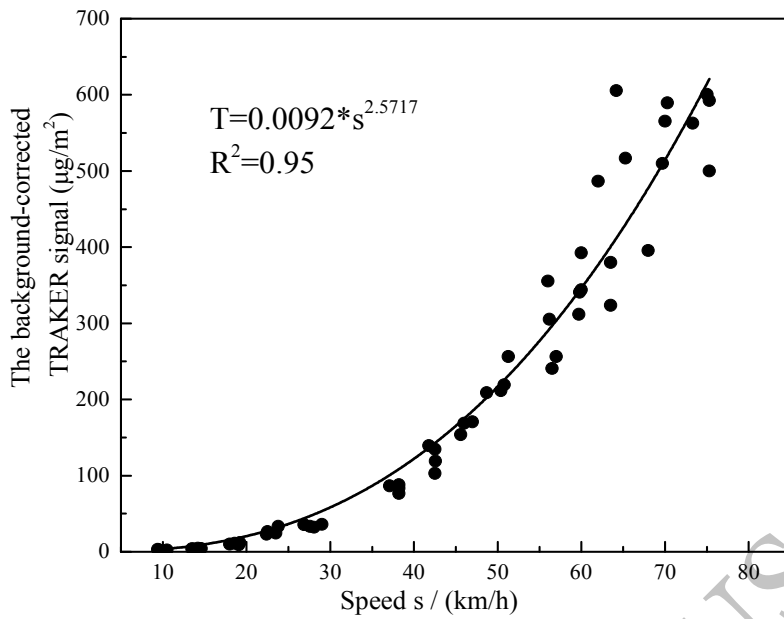
426
427
428
429
430
431
432
433
434
435
436
437
438
439
440
441
442
443
444
445
446
447
448
449
450
451



452

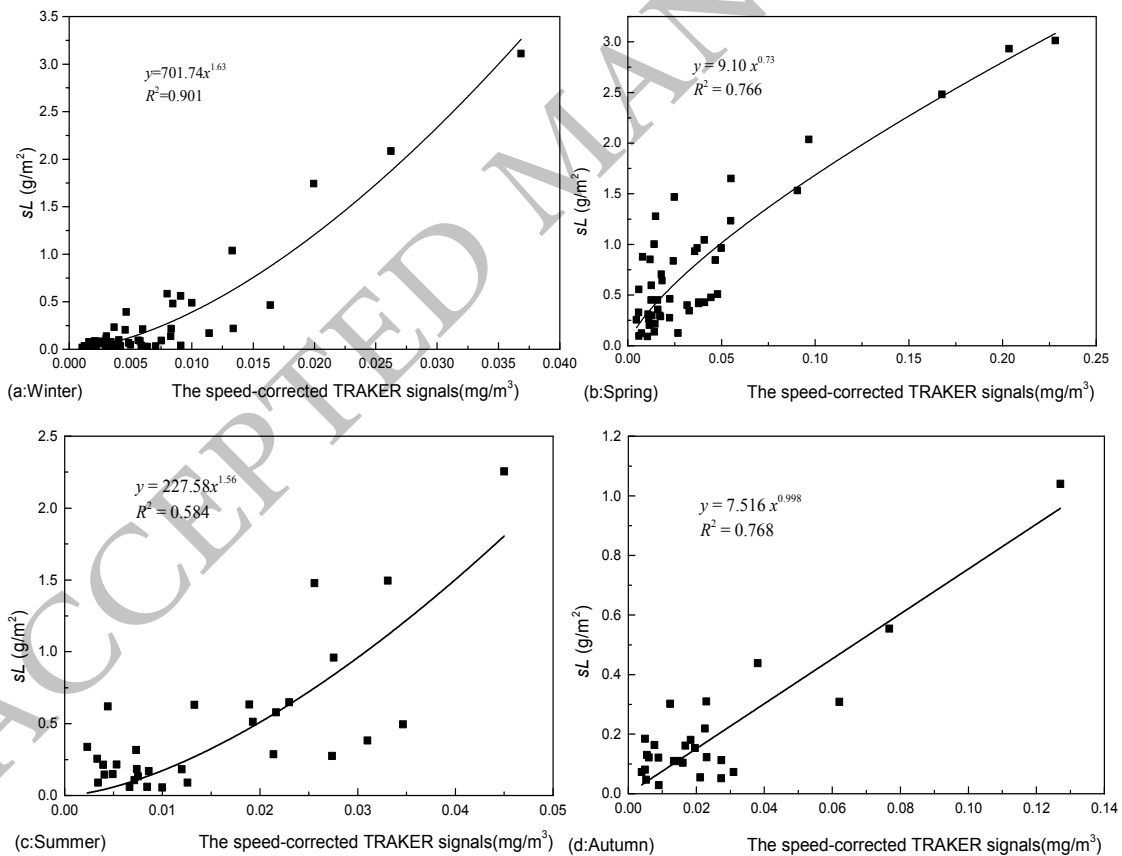
453

Figure 1 Configuration of the TRAKER vehicle instrument



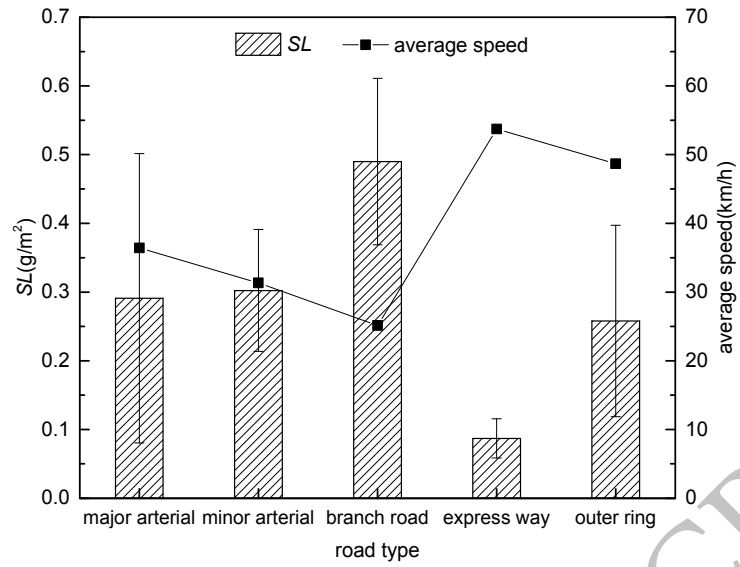
454

455 Figure 2 Relationship between vehicle speed and background-corrected TRAKER
456 signals



457

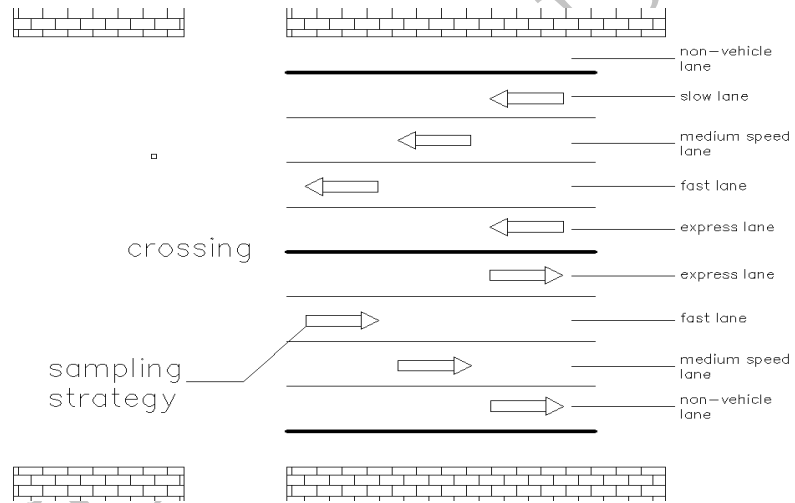
458 Figure 3 Relationship between the speed-corrected TRAKER signals and sL values



459

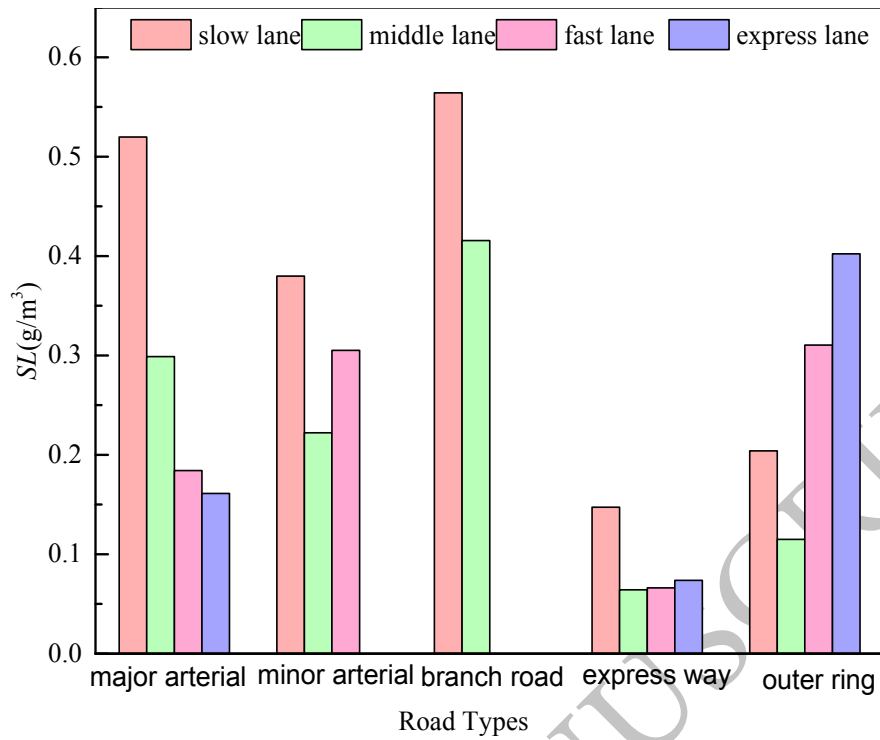
460 Figure 4 sL values by TRAKER and the average speed on different types of roads

461



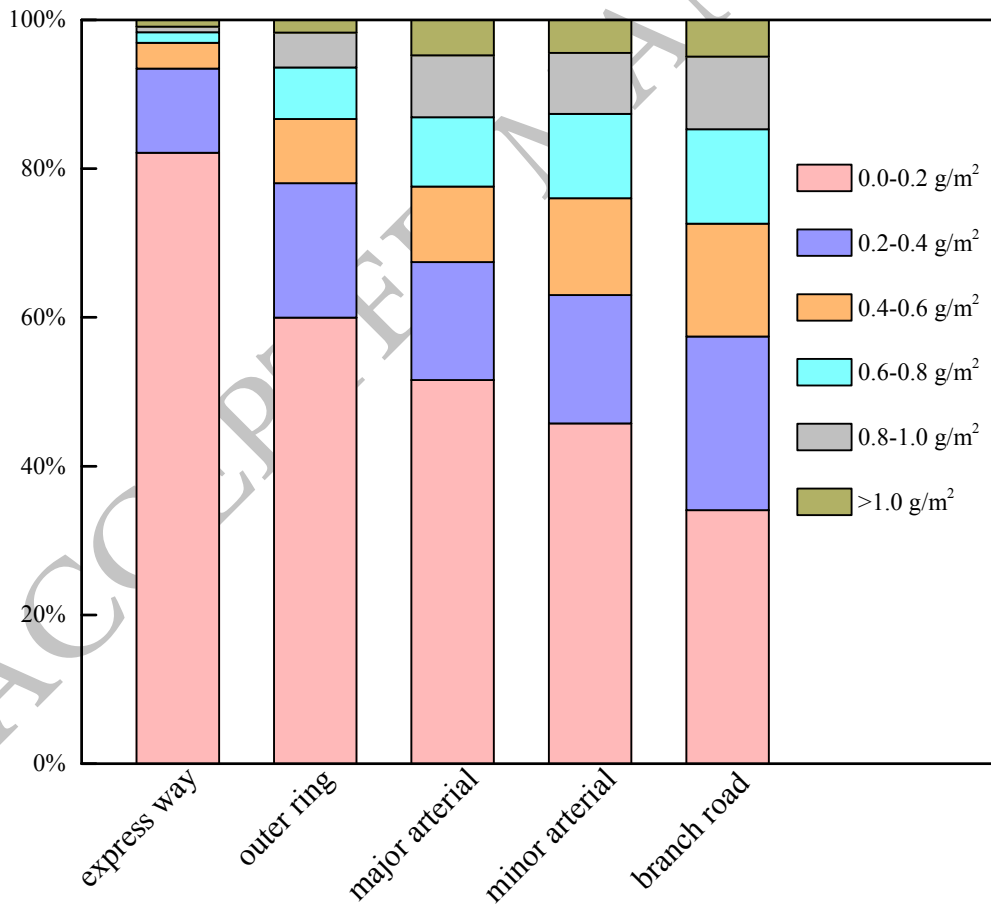
462

463 Figure 5 Schematic diagram of different vehicle lanes on roads in Tianjin



464

465 Figure 6 *sL* values by TRAKER in different lanes on various types of roads in Tianjin

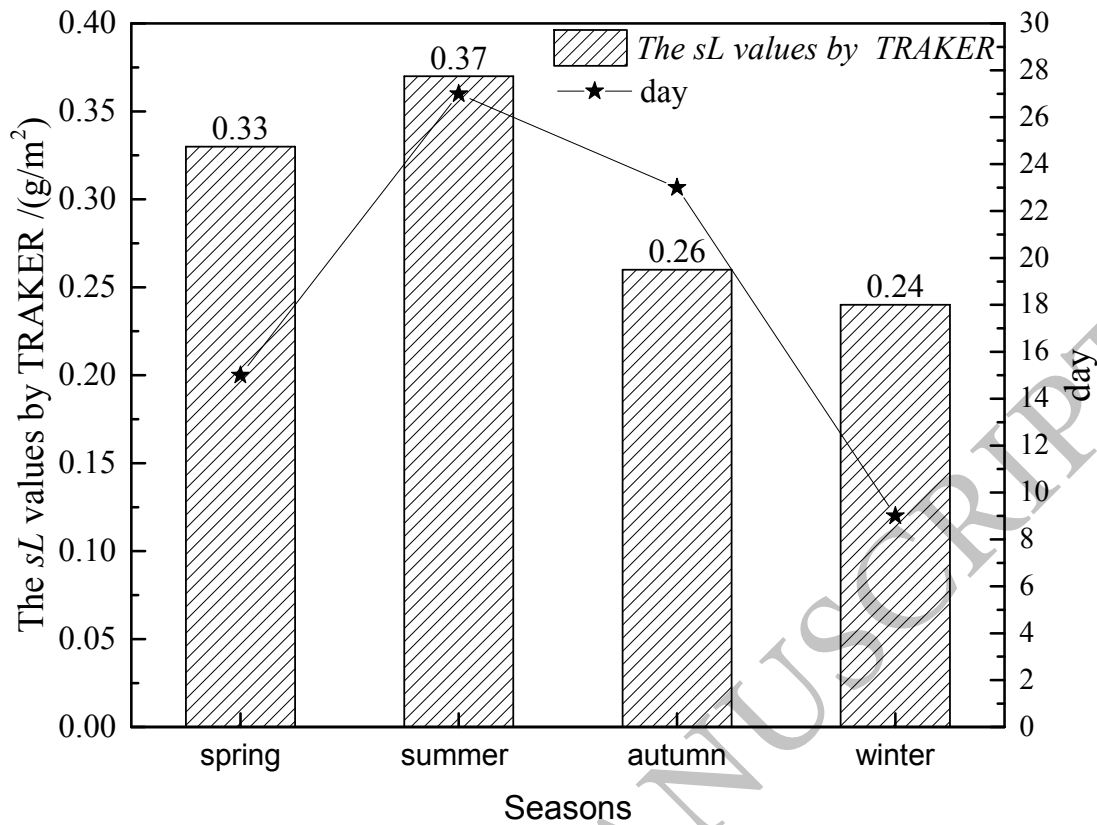


466

467 Figure 7 Frequency distribution of the *sL* values by TRAKER on different types of

468

roads



469

470 Figure 8 Comparison of the sL values by TRAKER and the rainfall days in different

471

472

Table 1 Details of roads sampled in this study

Road name	Road type	Road direction
Weijin road	Major arterial	South-north direction
Fukang road	Major arterial	East-west direction
Huanghe road	Minor arterial	East-west direction
Anshan west road	Minor arterial	East-west direction
Erwei road	Branch road	East-west direction
Baidi road	Branch road	South-north direction
Yingshui road	Branch road	East-west direction
Hongqi road	Expressway	East-west direction
Waihuan west road	Outer ring	South-north direction

473

474 Table 2 Traffic volume on various road types during sampling (unit: vehicles/day)

Road type	Major arterial	Minor arterial	Branch road	Expressway	Outer ring
Traffic volume	94,184	56,540	34,701	201,097	77,482

475